

^{11}B and ^{15}N solid state NMR investigation of a boron nitride preceramic polymer prepared by ammonolysis of borazine

Christel Gervais^{a,*}, Eric Framery^b, Christophe Duriez^c, Jocelyne Maquet^a,
Michel Vaultier^c, Florence Babonneau^a

^a *Laboratoire de Chimie de la Matière Condensée, UMR 7574, Université de Pierre et Marie Curie, 4 place Jussieu, T54-E5, F-75252 Paris, Cedex 05, France*

^b *Laboratoire de Méthodologie de Synthèse et Molécules Bioactives, UMR 5181, Université Claude Bernard Lyon 1, 43 bd du 11 novembre 1918, F-69622 Villeurbanne, Cedex, France*

^c *SESO, UMR 6510, Université de Rennes I, Campus de Beaulieu, Avenue du Général Leclerc, F-35042 Rennes, Cedex, France*

Available online 11 September 2004

Abstract

A poly(aminoborazine), precursor for hexagonal boron nitride (h-BN) obtained by reaction of borazine $\text{B}_3\text{N}_3\text{H}_6$ with ammonia, and its pyrolysis derivatives have been extensively characterised by ^{15}N and ^{11}B MAS NMR. The various B and N sites have been identified according to their first neighbouring atoms, as well as to the second ones in the case of ^{15}N , and have also been quantified. This study demonstrates that a suitable choice of NMR techniques together with the use of isotopic enrichment can lead to a large improvement in spectral resolution, which allows a better understanding of such complex BN preceramic polymer structures and permits to follow the polymer-to-ceramic transformation. © 2004 Elsevier Ltd. All rights reserved.

Keywords: Polymer; Ceramic; Solid State; NMR; Boron nitride; Poly(aminoborazine)

1. Introduction

Polymeric approach to refractory non oxide ceramics is a process of great interest offering possibilities of obtaining composite and shaped materials such as fibers, films or bulk pieces from soluble or fusible starting polymers.¹ It has first been developed to produce SiC or SiCN-based ceramics, starting from polysilanes, polycarbosilanes and polysilazanes.^{2,3} More recently, this approach was extended to the preparation of hexagonal boron nitride (h-BN), a ceramic widely used in high temperature technology.⁴ Different families of polymeric precursors have been developed by several groups, starting from borazine⁵ ($\text{B}_3\text{N}_3\text{H}_6$); or N- and B-substituted borazines.^{4,6–8}

While polyborazilene has proven to be an excellent precursor for the production of boron nitride coating, films and shaped materials, this cross-linked polymer appears less

adapted to applications requiring melt-processing due to the need to control the dehydrocoupling reactions. One strategy is to reduce the number of reactive BH and NH groups, by functionalising the polymer with suitable substituents as amines.⁹ A good knowledge of the structure of fusible polymers or copolymers seems to be the key to obtain BN fibers with high properties. It is therefore essential to control as much as possible the polymerisation and ceramisation steps and consequently to have effective characterisation tools that can follow the changes in local environments during polymer-to-ceramic conversion. Solid-state NMR studies have been shown to be extremely useful in this field and more particularly, ^{11}B and ^{15}N solid-state NMR techniques are particularly relevant to probe BN-based materials.^{10,11}

^{15}N is a spin 1/2 with a very low sensitivity in natural abundance (3.8×10^{-6} compared with ^1H) but this drawback may be overcome by ^{15}N enrichment and the use of Cross Polarisation (CP) techniques, taking advantage of the ^1H – ^{15}N dipolar coupling. These techniques are consequently very sensitive to the proton environment of the ni-

* Corresponding author.

E-mail address: gervais@ccr.jussieu.fr (C. Gervais).

trogen sites through the ^1H – ^{15}N distances and to molecular motion.

^{11}B is an abundant isotope (80.22%) but measurement of high-resolution spectra of this half-integer quadrupolar nucleus ($I = 3/2$) can be difficult because of the second order quadrupolar interaction which distorts the signals and can only be partially averaged by MAS.¹² Moreover, the ^{11}B chemical shift range observed in BN compounds is relatively small.¹³ Nonetheless, recording spectra at higher field permits to minimise the second order quadrupolar broadening since the intensity of the quadrupolar interaction is inversely proportional to the static field. Using different fields will also improve the confidence in the simulation of the resonance signals.

In this paper, we report therefore a detailed solid-state NMR characterisation of a poly(aminoborazine) obtained by reactions of borazine $\text{B}_3\text{N}_3\text{H}_6$ with ammonia and its pyrolysis derivatives. This polymer offers several advantages for the impregnation of matrices,¹⁴ and could be a good candidate in the formation of new generation BN fibers.

2. Experimental

2.1. Sample preparation

2.1.1. Poly(aminoborazine) $\text{POL}(\text{NH}_3)$

Under an atmosphere of dry nitrogen, 1.30 g (76.5 mmol) of NH_3 (Alphagaz, 3.6 nv) were condensed at -80°C in a reactor. When the temperature was warmed to -40°C , 2.00 g (25.0 mmol) of ^{15}N -enriched borazine were added. A quick one-step procedure to obtain borazine from sodium borohydride NaBH_4 and ammonium sulfate $(\text{NH}_4)_2\text{SO}_4$ was recently proposed.¹⁵ The ^{15}N enriched polymer was obtained from enriched borazine synthesized with ammonium sulfate ^{15}N enriched at 10 at.% purchased from Isotec. The mixture was warmed to room temperature in 1 h. The crude was only composed of a white powder, dried under vacuum (0.05 mmHg) to remove the trace of borazine. 2.90 g of a white solid were collected (88% weight yield). The isotopic enrichment was evaluated by mass spectrometry and was estimated to 10%. The structure of this poly(aminoborazine) polymer is compared to a polyborazilene $\text{POL}(\Delta)$ prepared by a procedure proposed in the literature¹⁶ that consists in thermal dehydropolymerisation of borazine. Pyrolysis of these polymers was then performed by inserting a quartz tube loaded in the glovebox and equipped with a dried argon gas flow into a tubular furnace. The heating rate was $10^\circ\text{C}/\text{min}$.

2.2. NMR experiments

^{15}N CP MAS experiments were performed at room temperature on a Bruker MSL-300 spectrometer, at a frequency of 30.41 MHz (^{15}N) and 300.13 MHz (^1H), using a Bruker CP-MAS probe. Solid samples were spun at 5 kHz, using

7 mm ZrO_2 rotors filled up in a glovebox under dried argon atmosphere. All ^{15}N CP MAS experiments were performed under the same Hartmann-Hahn match condition, set up by using a powdered sample of NH_4NO_3 : both RF channel levels $\omega_{^1\text{H}}/2\pi$ and $\omega_{^{15}\text{N}}/2\pi$ were carefully set so that $|\omega_{^1\text{H}}|/2\pi = |\omega_{^{15}\text{N}}|/2\pi = 42\text{ kHz}$. Proton decoupling was always applied during acquisition and a repetition time of 10 s was used. The ^{15}N Single Pulse Experiment (SPE) MAS NMR spectra were recorded with a pulse angle of 90° and a recycle delay between pulses of 100 s. Chemical shifts were referenced to solid NH_4NO_3 (10% ^{15}N enriched sample, $\delta_{\text{iso}}(^{15}\text{NO}_3) = -4.6\text{ ppm}$ compared to CH_3NO_2 ($\delta = 0\text{ ppm}$)).

^{11}B MAS NMR experiments were performed at room temperature on a Bruker MSL-400 spectrometer, at a frequency of 128.28 MHz, using a Doty CP-MAS probe with no probe background. Solid samples were spun at 10 kHz, using 5 mm ZrO_2 rotors filled up in a glovebox under dried argon atmosphere. ^{11}B MAS experiments were also performed at 18.8 T on a Bruker DSX800 spectrometer using 4 mm ZrO_2 rotors. A $1\ \mu\text{s}$ single-pulse excitation (while the t_{90° measured on BF_3OEt_2 is $8\ \mu\text{s}$) was employed, with repetition times of 5 s. All ^{11}B chemical shifts were determined relative to liquid BF_3OEt_2 ($\delta = 0\text{ ppm}$). Spectra were simulated using the DM-FIT program.¹⁷

3. Results

3.1. Chemical analysis

The results of the elemental analysis of the samples pyrolysed at various temperatures are summarised in Table 1 and were obtained from Service Central d'Analyse du CNRS (Vernaison, France). The poly(aminoborazine) $\text{POL}(\text{NH}_3)$ exhibits a higher degree of protonation than $\text{POL}(\Delta)$ prepared by thermal dehydropolymerisation of borazine, suggesting a smaller degree of crosslinking. Moreover, the molar ratio N/B remains fairly constant with temperature and the main evolution observed is a deprotonation of the system. Finally, it is worth noticing that, from 200°C , compositions of the two systems become quite close.

Table 1
Chemical analysis data and molar compositions of the polymers heat-treated at different temperatures

Pyrolysis temperature ($^\circ\text{C}$)	Element (wt.%)			Empirical formula
	B (± 0.2)	N (± 2)	H (± 0.1)	
$\text{POL}(\text{NH}_3)$	33.6	45.0	9.5	$\text{B}_{1.0}\text{N}_{1.1}\text{H}_{3.1}$
200	29.8	50.0	4.8	$\text{B}_{1.0}\text{N}_{1.1}\text{H}_{1.7}$
400	34.3	50.5	3.1	$\text{B}_{1.0}\text{N}_{1.1}\text{H}_{1.0}$
600	35.1	59.0	1.8	$\text{B}_{1.0}\text{N}_{1.3}\text{H}_{0.5}$
$\text{POL}(\Delta)$	37.6	53.2	5.1	$\text{B}_{1.0}\text{N}_{1.1}\text{H}_{1.5}$
200	31.3	55.5	3.7	$\text{B}_{1.0}\text{N}_{1.3}\text{H}_{1.3}$
400	29.8	50.8	3.4	$\text{B}_{1.0}\text{N}_{1.3}\text{H}_{1.2}$
800	38.6	55.0	1.2	$\text{B}_{1.0}\text{N}_{1.1}\text{H}_{0.3}$
1450	42.7	54.1	0.2	$\text{B}_{1.0}\text{N}_{1.0}\text{H}_{<0.05}$

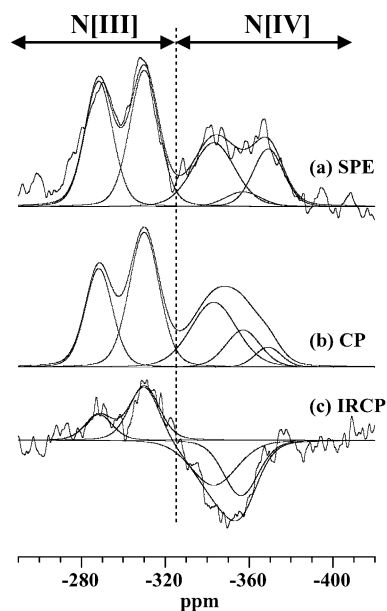


Fig. 1. ^{15}N MAS NMR spectra of $\text{POL}(\text{NH}_3)$ (a) SPE spectrum; (b) CP spectrum (contact time: 5 ms); and (c) IRCP spectrum (contact time: 5 ms; inversion time: 125 μs).

3.2. Pre-ceramic polymer

3.2.1. ^{15}N NMR study

The ^{15}N SPE MAS NMR spectrum of $\text{POL}(\text{NH}_3)$ (Fig. 1(a)) shows a composite signal in which two domains in chemical shift can be distinguished: from -250 to -330 ppm for tricoordinated N atoms N[III] and from -330 to -400 ppm for tetracoordinated N atoms N[IV].¹⁸ $\text{POL}(\Delta)$ consists only of N[III] sites at -257 , -268 , -284 , -294 , -302 , -311 and -326 ppm¹⁰ while $\text{POL}(\text{NH}_3)$ presents a large distribution of N[III] and N[IV] sites. An elegant way to assign more precisely the various N sites with the same coordination number is the use of the Inversion Recovery Cross Polarisation (IRCP) technique^{19,20} permitting to distinguish the N sites from their proton environments. This sequence has already been successfully used to identify $^{15}\text{NH}_x$ sites ($x = 0-3$) in aminoboranes¹³ and in $\text{POL}(\Delta)$.¹⁰ IRCP MAS NMR spectra of $\text{POL}(\text{NH}_3)$ were thus recorded for various inversion times t_i ranging from 5 μs to 1 ms (Fig. 1). All the signals are inverted for $t_i = 1$ ms as observed in $\text{POL}(\Delta)$. Nonetheless, it is clear that all the individual components do not invert at the same rate. We have tried to simulate all the spectra with a single set of peaks, by keeping the chemical

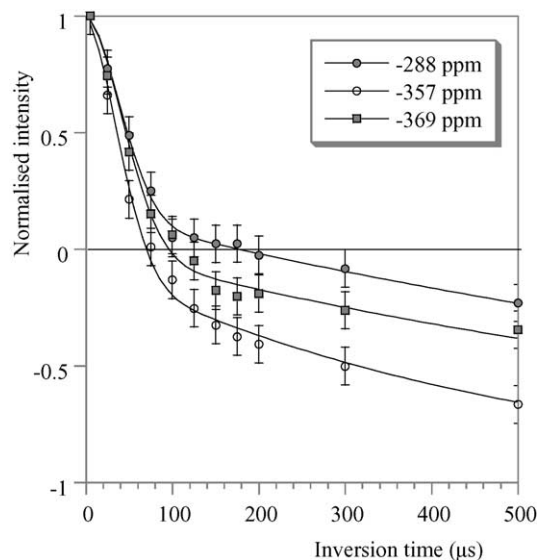


Fig. 2. Evolution vs. inversion time of the ^{15}N IRCP MAS NMR signal intensities of different sites of the polymer $\text{POL}(\text{NH}_3)$ (solid lines correspond to the simulations according to Eq. (1)).

shifts, linewidths and shapes constant and by fitting only the amplitudes for each spectra. It was necessary to introduce six peaks in order to reproduce the shape of the spectra for each inversion time (Fig. 1). The integrated intensities of each signal were then normalised and plotted against inversion time. The resulting polarisation curves show a two-regime inversion behaviour with a rapid decrease of the magnetisation at low inversion time (Fig. 2). They can thus be interpreted within the frame of the I*-I-S model,²¹ where strongly coupled I-S spin pairs interact with an abundant I* spin reservoir through homonuclear I-I* dipolar coupling. In that case, the polarisation inversion behaviour can be simulated with the following equation:^{19,20}

$$M_S(t_i) = M^0(t_c) \left[\frac{2}{n+1} \exp\left(-\frac{t_i}{T_D}\right) + \frac{2n}{n+1} \exp\left(-\frac{3t_i}{2T_D}\right) \exp\left(-\frac{t_i^2}{T_C^2}\right) - 1 \right] \quad (1)$$

where T_C is related to dipolar coupling to nearby protons (I-S) leading to a coherent transfer of polarisation,²² T_D describes the decay caused by isotropic spin diffusion between I and I* spins ($T_C \ll T_D$) and n corresponds to the number of strongly coupled protons. The results of the simu-

Table 2
CP characteristic times of $\text{POL}(\text{NH}_3)$ signals extracted from the ^{15}N IRCP MAS spectra

δ_{iso} (ppm) (± 1)	T_C (μs) (± 2)	T_D (ms) (± 0.1)	t_i^0 (μs) (± 10)	n (± 0.5)	Proportions ($\pm 2\%$)	Assignment
-288	55	1.1	160	0.7	28	NHB ₂
-309	57	1.0	170	0.7	32	NHB ₂
-343	55	0.5	70	1.0	22	NH ₂ B ₂
-357	56	0.5	70	1.1	4	NH ₂ B ₂
-369	62	1.0	85	0.9	14	NH ₃ B

Assignment and partition of these sites extracted from the simulation of the ^{15}N SPE MAS spectrum.

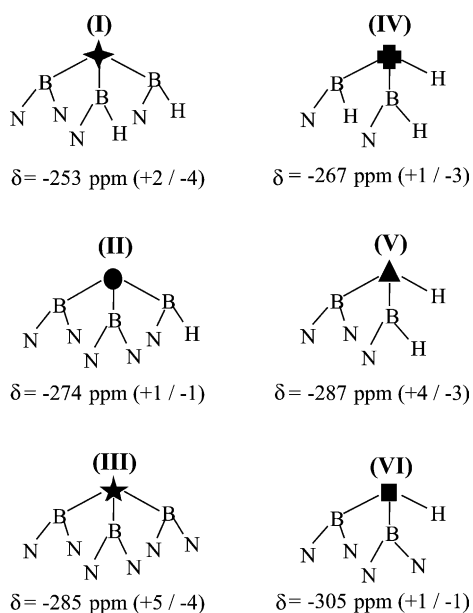


Fig. 3. Schematic representations and calculated ^{15}N chemical shifts of nitrogen environments in hydrogen-saturated cut-outs of h-BN according to first and second coordination spheres.²³

lation are summarised in Table 2. The observed T_C values are quite similar for all the detected ^{15}N sites, and close to those observed for protonated nitrogen environments¹³ suggesting for each detected site, the existence of a strong ^{15}N – ^1H heteronuclear dipolar coupling. Moreover, signals appearing at -288 and -309 ppm show inversion time values t_1^0 (corresponding to a magnetisation equal to zero) very similar to those observed for NHB_2 sites in $\text{POL}(\Delta)$. A more precise assignment of both sites can be proposed according to ab initio calculations performed by Gastreich and Marian on model clusters²³ and proposing six distinct ^{15}N chemical shift values for tricoordinated N sites with different first and/or second neighbouring atoms (Fig. 3). The signals at -288 and -309 ppm could therefore be tentatively attributed to (V) and (VI) environments. Signals at -343 and -357 ppm exhibit much shorter inversion time values t_1^0 and their chemical shift values strongly suggest NB_2H_2 environments while the site at -369 ppm has a position typical of a B-NH_3 .¹³ Regarding the IRCP behaviour of this last signal, the observed dynamics can be explained by the mobility of the NH_3 group partially averaging the ^1H – ^{15}N dipolar interaction.

It can be noticed that no NB_3 signals could be clearly identified: this is in good agreement with the comparison between quantitative SPE and CP MAS spectra (Fig. 1(a) and (b)) showing very similar tricoordinated signals proportions. Unprotonated NB_3 signals would be more intense in the SPE spectrum and underestimated at short contact times optimised for protonated N.²⁴ It strongly suggests that the amount of NB_3 environments is very small. The percentages of the various sites extracted from the simulation of the quantitative SPE MAS spectrum are summarised in Table 2.

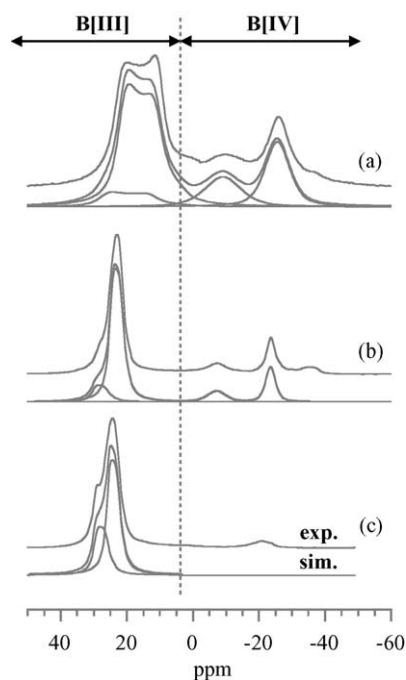


Fig. 4. Experimental and simulated ^{11}B MAS NMR spectra of (a) $\text{POL}(\text{NH}_3)$ recorded at 9.4 T; (b) $\text{POL}(\text{NH}_3)$ recorded at 18.8 T; and (c) $\text{POL}(\Delta)$ recorded at 18.8 T.

3.2.2. ^{11}B NMR study

The ^{11}B MAS NMR spectrum of $\text{POL}(\text{NH}_3)$ recorded at 9.4 T (Fig. 4(a)) shows two chemical shift ranges corresponding to tricoordinated B[III] atoms (from 0 to 40 ppm) and to tetracoordinated B[IV] atoms (from -40 to 0 ppm). Two sites around -10 and -25 ppm can be clearly identified among B[IV] atoms and assigned to BN_2H_2 and BNH_3 .¹⁸ The deconvolution of the B[III] sites is more difficult because of the large quadrupolar interaction that broadens the peak over a large chemical shift range. To overcome this problem, the ^{11}B MAS spectrum of the polymer was recorded at 18.8 T (Fig. 4(b)). The quadrupolar interaction scales indeed inversely proportional to the applied magnetic field so is reduced at higher fields.²⁵ In the area of B[III] sites, the spectrum recorded at 18.8 T shows two signals at 27 ppm ($C_Q = 2.7$ MHz, $\eta = 0.1$) and 31 ppm ($C_Q = 2.9$ MHz, $\eta = 0.1$) that can be attributed to BN_3 and BN_2H sites, respectively, by comparison with previously obtained results on $\text{POL}(\Delta)$ ¹⁰ (Fig. 4(c)). The extracted percentages of the different boron sites are summarised in Table 3.

Table 3

Proportions of the different boron sites obtained from the simulation of the ^{11}B MAS spectra of $\text{POL}(\text{NH}_3)$

δ_{iso} (ppm) (± 2)	C_Q (MHz) (± 0.1)	η (± 0.1)	Proportions (%) (± 2)	Attribution
31	2.9	0.1	10	BHN_2
27	2.7	0.1	60	BN_3
-12	–	–	13	BH_2N_2
-22	–	–	17	BH_3N

As a conclusion regarding the structure of POL(NH₃), the BN₃/BHN₂ ratio is estimated at 85/15 suggesting that the cross-linking of the borazine occurs predominantly by the boron atoms of the cycle as confirmed by the very small amount of NB₃ environments detected. The B^{III}/B^{IV} and N^{III}/N^{IV} ratios are estimated at 70/30 and 60/40 respectively. The polymer appears richer in B^{III} and N^{III} atoms than in B^{IV} and N^{IV} atoms, indicating that the linear polyaminoborane (NH₂–BH₂)_n parts should be short. This suggests that the main step of the polymerisation process is the complexation of boron atoms of borazine with 1, 2 or 3 molecules of NH₃, then followed immediately by two rearrangements: (i) borazine ring opening leading to the formation of borane–ammonia complex NH₃·BH₃ and polyaminoboranes –NH₂–BH₂– groups; and (ii) the formation of B-aminoborazines. During these rearrangements, the exchange of nitrogen atoms of borazine cycle with the nitrogen atoms of ammonia could not be excluded as described by Paine and co-workers.²⁶ Borazanaphthalene B₅N₅H₈ and different borazine ring derivatives connected by short linear polyaminoboranes (NH₂–BH₂)_n chains could then be obtained from B-aminoborazine derivatives via successive reactions with NH₃ and the different sources of BH₃ such as NH₃·BH₃.

The structure of the polymers suggested by the distribution of the different nitrogen and boron environments is presented in Fig. 5. It shows short linear polyaminoborane chains between borazine groups with a very small amount of borazanaphthalene or more polycondensed borazine cycles.

3.3. Pyrolysis products

3.3.1. ¹⁵N NMR study

The ¹⁵N MAS NMR spectra recorded for the POL(NH₃) and its pyrolysis products up to 600 °C are presented in Fig. 6. Interestingly, it can be noticed that from 200 °C, all tetracoordinated N[IV] sites have disappeared and only N[III] sites remain. At 600 °C, a main signal corresponding to an NB₃ environment in h-BN is observed at –284 ppm.^{10,23} To precise the site attributions, a series of IRCP spectra were run in order to distinguish the N sites from their proton environments.

200 °C: It was necessary to introduce four peaks in order to reproduce the shape of the various IRCP MAS NMR spectra for each inversion time. Two of them at –270 and –284 ppm inverse quite slowly and can therefore be assigned to NB₃ sites while the other two at –294 and –306 ppm are already inverted for an inversion time of 150 μs and exhibit an inversion dynamic characteristic of NHB₂ environments. These assignments are in good agreement with ab initio calculations²³ and these different sites at –270, –284, –294 and –306 ppm can more precisely be attributed to (II), (III), (V) and (VI) environments (Fig. 3).

400 °C: The ¹⁵N MAS NMR spectrum of the polymer pyrolysed at 400 °C (Fig. 6(b)) is relatively similar to the one obtained for the sample heat-treated at 200 °C (Fig. 6(a)) with a higher proportion of sites appearing at smaller chemical shift values and corresponding to NB₃ sites. This is in good agreement with a progressive deprotonation with temperature.

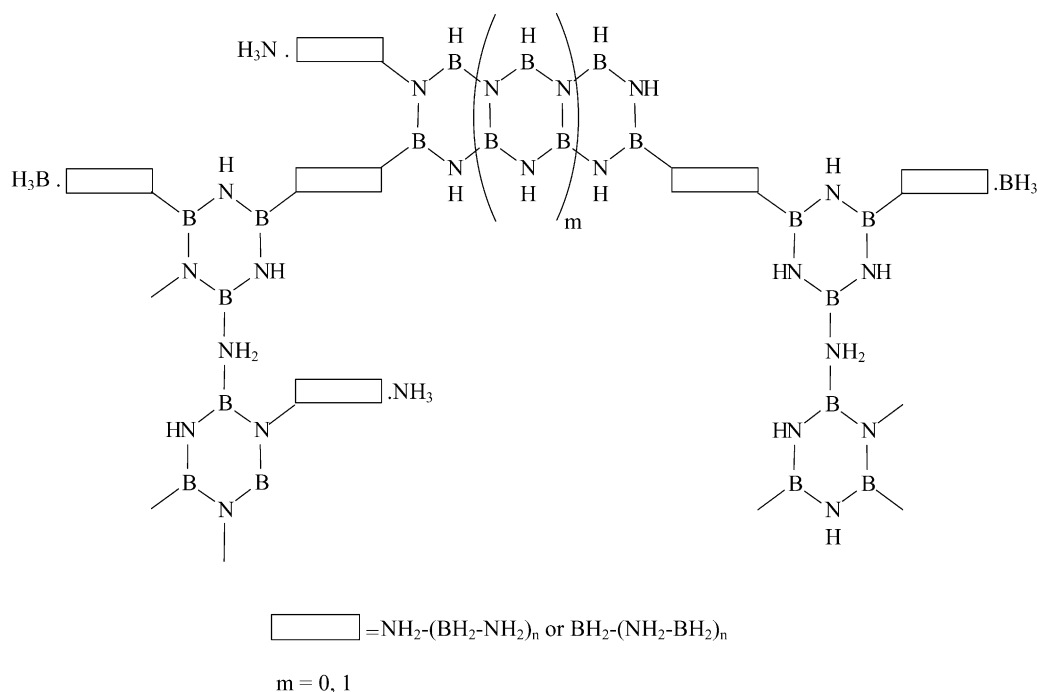


Fig. 5. Proposed structure for the poly(aminoborazine) POL(NH₃) considering the results of the ¹¹B and ¹⁵N NMR study.

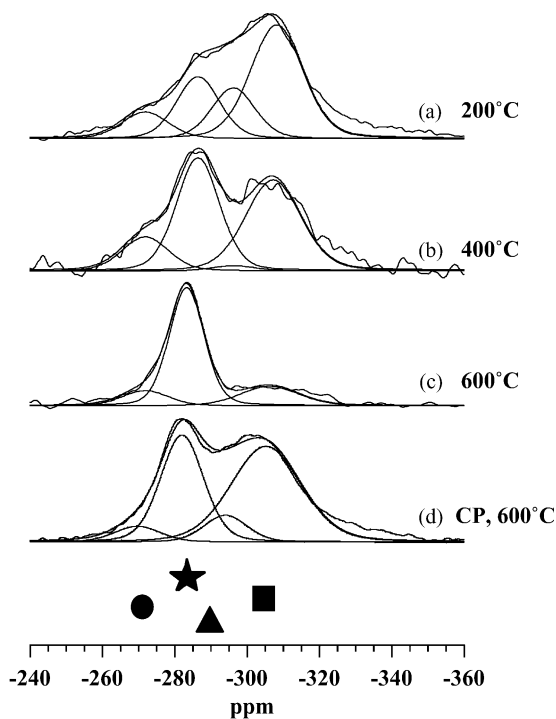


Fig. 6. Experimental and simulated ^{15}N MAS NMR spectra of $\text{POL}(\text{NH}_3)$ heat-treated at (a) 200 °C; (b) 400 °C; (c) 600 °C; and (d) ^{15}N CP MAS spectrum of $\text{POL}(\text{NH}_3)$ heat-treated at 600 °C (contact time: 5 ms). Symbols added refer to the position of different nitrogen environments described in Fig. 3.

600 °C: This sample shows a ^{15}N MAS spectrum (Fig. 6(c)) dominated by a signal at –284 ppm and assigned to an environment of type (III) characteristic of h-BN. But the ^{15}N CP MAS spectrum (Fig. 6(d)) clearly shows an additional signal at –306 ppm. The obvious overestimation of this signal by the CP experiment confirms that it corresponds to an NHB_2 environment of type (VI) in good agreement with the previous proposed assignment. An additional signal at –270 ppm also present at 200 and 400 °C can be assigned to a type (II) environment. The main NB_3 signal is very similar to the one observed in h-BN while the two other sites evidenced, NB_3 (II) and NHB_2 (VI), exhibit only one proton up to the second coordination sphere.

The ^{15}N SPE MAS spectra of the samples heat-treated at 200, 400 and 600 °C (Fig. 6) were then simulated using the different sites extracted from the IRCP and the percentages of the various sites extracted from these simulations are summarised in Table 4.

3.3.2. ^{11}B NMR study

The ^{11}B MAS NMR spectra recorded for the polymer and its pyrolysis products up to 600 °C (Fig. 7) show that similarly to what was observed by ^{15}N NMR, all tetracoordinated B[IV] sites have disappeared from 200 °C and all spectra appear quite similar at first sight with a shape characteristic of

Table 4

Proportions of the different nitrogen sites obtained from the simulation of the ^{15}N SPE MAS spectra of the $\text{POL}(\text{NH}_3)$ heat-treated at 200, 400 and 600 °C

δ_{iso} (ppm) (± 2)	Proportions (%) (± 2)			Attribution
	200 °C	400 °C	600 °C	
–270	10	13	12	NB_3 (II)
–284	22	42	69	NB_3 (III)
–294	18	2	–	NHB_2 (V)
–306	50	43	12	NHB_2 (VI)

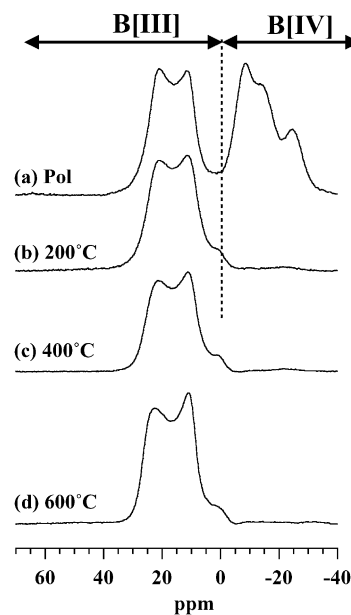


Fig. 7. ^{11}B MAS NMR spectra recorded at 9.4 T of (a) $\text{POL}(\text{NH}_3)$ and its pyrolysis products at (b) 200 °C; (c) 400 °C; and (d) 600 °C.

tricoordinated boron atoms engaged in a B_3N_3 six-membered ring structure²⁷ ($\delta \approx 30$ ppm, $C_Q \approx 2.8$ MHz, $\eta \approx 0$). As previously described, two type of sites corresponding to BN_3 ($\delta = 27$ ppm, $C_Q = 2.7$ MHz, $\eta = 0.1$) and BN_2H ($\delta = 31$ ppm, $C_Q = 2.9$ MHz, $\eta = 0.1$) are more particularly expected. A precise simulation is difficult at this field but the main tendency is a large decrease of the intensity of the BHN_2 signal with temperature.

This result is in good agreement with ^{15}N experiments and confirms that the ceramisation process of $\text{POL}(\text{NH}_3)$ leading to h-BN occurs through a preferential disappearance of B–H linkages. The residual protonated nitrogen site (VI) identified at 600 °C show indeed no B–H bonds.

4. Conclusion

A range of ^{11}B and ^{15}N solid-state NMR techniques have been used to investigate in details the structure of a poly(aminoborazine) obtained from ammonolysis of borazine and follow its ceramisation process. Combination

of ^1H – ^{15}N cross-polarisation sequences and ^{15}N enrichment allows us to distinguish various N sites, revealing the high sensitivity of this isotope not only to the first, but also to the second neighbouring atoms. Environments were proposed based on the comparison between the experimental chemical shift values and ab initio calculations already reported in the literature. The ^{11}B chemical shift values are much less sensitive to differences in first neighbouring atoms. Furthermore, the second order quadrupolar broadening renders quite difficult the interpretation of the spectra unless recording spectra at a very high field.

Surprisingly, this polymer contains both tri- and tetracoordinated boron and nitrogen atoms, present in four types of B sites (BHN_2 , BN_3 , BH_2N_2 , BNH_3) and three types of N sites (NHB_2 , NH_2B_2 , NBH_3), if only the first neighbouring atoms are considered. This suggests rearrangement reactions and more particularly borazine ring opening leading to the formation of borane–ammonia complex $\text{NH}_3\cdot\text{BH}_3$ and polyaminoboranes $-\text{NH}_2-\text{BH}_2-$ groups. Quantitative analysis gives the following estimations: $\text{BHN}_2/\text{BN}_3 = 15/85$, $\text{B}^{\text{III}}/\text{B}^{\text{IV}} = 70/30$ and $\text{N}^{\text{III}}/\text{N}^{\text{IV}} = 60/40$ suggesting a structure of relatively small polyaminoborane chains linked to borazine groups by the boron atoms of the rings.

The polymer-to-ceramic transformation was then followed through the study of samples pyrolysed at selected temperatures. Due to the large sensitivity of the ^{15}N chemical shift values, a good picture of the change in N environments could be obtained from the ^{15}N MAS NMR spectra: it suggests that the ceramisation process leading to h-BN occurs through a preferential disappearance of B–H bonds.

Acknowledgments

The authors would like to acknowledge S. Steuernagel (Bruker, Karlsruhe, Germany) and D. Massiot (CRMHT, Orléans, France) for their help in recording the ^{11}B MAS NMR spectra at 18.8 T.

References

1. Bill, J. and Aldinger, F., *Adv. Mater.*, 1995, **7**, 775.
2. Birot, M., Pillot, J.-P. and Dunogues, J., *Chem. Rev.*, 1995, **95**, 1443.
3. Laine, R. M. and Babonneau, F., *Chem. Mater.*, 1993, **5**, 260.
4. Paine, R. T. and Narula, C. K., *Chem. Rev.*, 1990, **90**, 73.
5. Fazen, P. J., Remsen, E. E., Beck, J. S., Carrol, P. J., McGhie, A. R. and Sneddon, L. G., *Chem. Mater.*, 1995, **7**, 1942.
6. Seyferth, D. and Rees Jr., W. S., *Chem. Mater.*, 1991, **3**, 1106.
7. Moon, K.-T., Min, D.-S. and Kim, D.-P., *Bull. Korean Chem. Soc.*, 1998, **19**, 222.
8. Cornu, D., Miele, P., Faure, R., Bonnetot, B., Mongeot, H. and Bouix, J., *J. Mater. Chem.*, 1999, **9**, 757.
9. Wideman, T., Remsen, E. E., Cortez, E., Chlanda, V. L. and Sneddon, L. G., *Chem. Mater.*, 1998, **10**, 412.
10. Gervais, C., Maquet, J., Babonneau, F., Duriez, C., Framery, E., Vaultier, M. et al., *Chem. Mater.*, 2001, **13**, 1700.
11. Gervais, C. and Babonneau, F., *J. Organometallic Chem.*, 2002, **657**, 75.
12. Smith, M. E. and van Eck, E. R. H., *Prog. NMR Spectrosc.*, 1999, **34**, 159.
13. Gervais, C., Babonneau, F., Maquet, J., Bonhomme, C., Massiot, D., Framery, E. et al., *Magn. Reson. Chem.*, 1998, **36**, 407.
14. Parlier, M., Ropars, M., Vaultier, M., Framery, E., Jouin, J.-M. and Cavalier, J.-C., *World Patent*, 1998, **98**, 29355.
15. Wideman, T. and Sneddon, L. G., *Inorg. Chem.*, 1995, **34**, 1002.
16. Fazen, P. J., Beck, J. S., Lynch, A. T., Remsen, E. E. and Sneddon, L. G., *Chem. Mater.*, 1990, **2**, 96.
17. Massiot, D., Fayon, F., Capron, M., King, I., Le Calve, S., Alonso, B. et al., *Magn. Reson. Chem.*, 2002, **40**, 70.
18. Framery, E. and Vaultier, M., *Heteroat. Chem.*, 2000, **11**, 218.
19. Wu, X. and Zilm, K. W., *J. Magn. Reson. A*, 1993, **102**, 205.
20. Sangill, R., Rastrup-Andersen, N., Bildsoe, H., Jakobsen, H. J. and Nielsen, N. C., *J. Magn. Reson.*, 1994, **107**, 67.
21. Müller, L., Kumar, A., Baumann, T. and Ernst, R. R., *Phys. Rev. Lett.*, 1974, **32**, 1402.
22. Hirschinger, J. and Hervé, M., *Solid State NMR*, 1994, **3**, 121.
23. Gastreich, M. and Marian, C. M., *J. Comp. Chem.*, 1998, **19**, 716.
24. Snape, C. E., Axelson, D. E., Botto, R. E., Delpuech, J. J., Tekely, P., Gerstein, B. C. et al., *Fuel*, 1989, **68**, 54.
25. Massiot, D., Montouillout, V., Magnenet, C., Coutures, J.-P., Forster, H., Steuernagel, S. et al., *C. R. Acad. Sci. Paris (Série II)*, 1998, **1**, 157.
26. Rye, R. R., Tallant, D. R., Borek, T. T., Lindquist, D. A. and Paine, R. T., *Chem. Mater.*, 1991, **3**, 286.
27. Marchetti, P. S., Kwon, D., Schmidt, W. R., Interrante, L. V. and Maciel, G. E., *Chem. Mater.*, 1991, **3**, 482.